Unified Model of Skewed Aperture Ambient Light and Environmental Stabilization

Mostafa Nasr*[1]

[1]Independent Researcher, Giza, Egypt

September 15, 2025

Abstract

This paper presents a unified model for predicting ambient environmental conditions through skewed (non-orthogonal) apertures in buildings. The objective is to integrate lighting, thermal, and acoustic transmission into a single theoretical framework. We develop a formal model of light propagation through rotated or sheared apertures, decomposing incoming ambient illumination into a set of discrete directional components. Experimental validation is conducted using a custom test bench. Multi-sensor measurements show that model predictions of indoor illuminance and SPL are within 10 % of measured values, while thermal predictions are within 15 %. Coefficients of determination (R^2) are ≈ 0.85–0.90 ($p < 0.01$). A seven-direction basis approximates diffuse light and heat entering through a skewed aperture with minimal error.

1 Introduction

Motivation and prior art (daylighting anisotropy, acoustic transmission through apertures, passive solar gains). Contributions: a directional, multi-domain model with experimental validation. Prior studies on directional sky models and building apertures motivate our seven-source basis and multiplicative modifiers [1, 2]. Related acoustic and thermal transmission literature supports the unified treatment [3, 4].

2 Theoretical Framework

We define the aperture orientation by yaw ϕ and tilt ψ; shear parameters κ_x, κ_y capture edge skew. Figure 1 illustrates frames and the aperture solid-angle view.

Escape integral (light). The transmitted illuminance is

$$E_{\text{escape}} = \iint_{\Omega_{\text{ap}}} L_{\text{in}}(\theta, \varphi)\, \cos\theta \, \mathrm{d}\Omega. \tag{6}$$

*ORCID: 0009-0007-0753-6341

Multiplicative modifiers. Real-world effects (occlusion, transmissivity, internal reflectance) enter as

$$\tilde{E}_{\text{escape}} = \sum_i I_i \, \cos\theta_i \, T_i \, \prod_k M_{k,i}, \tag{7}$$

where $M_{k,i}$ are fitted modifier factors for source i.

Seven-source decomposition. Approximating the hemisphere by seven directions (zenith + six azimuthal):

$$E_{\text{escape}} \approx \sum_{i=1}^{7} I_i \, \cos\theta_i \, T_i. \tag{8}$$

Glint amplification. Grazing angles increase gain; we adopt a Fresnel-style factor

$$G_{\text{glint}}(\theta) = 1 + F_0 \, (\sec\theta - 1), \tag{9}$$

applied to glint-active directions (optionally restricted by a set $\mathcal{G}$).

3 Model Extensions: Two Incorporations

We incorporate two new ideas into the framework to broaden scope and practical impact:

- Incorporation I (Blueband spectral extension): a spectral weighting to emphasise short-wavelength content ("blueband") relevant to circadian and ecological responses.
- Incorporation II (Micro-environment testbeds): a dynamic, lumped-parameter thermal formulation for backyard/urban micro-labs and bio-digital feedback experiments.

Incorporation I: Blueband Spectral Extension

Let $L(\theta, \varphi, \lambda)$ be spectral radiance and $T(\lambda)$ the spectral transmissivity of the aperture/material stack for a given direction. Define a unit-normalised blueband weight $W_B(\lambda)$ (peaked near 460 nm to 490 nm). The blueband irradiance entering the space is

$$E_B \;\approx\; \sum_{i=1}^{7} \cos\theta_i \int_\lambda L_i(\lambda) \, T_i(\lambda) \, W_B(\lambda) \, \mathrm{d}\lambda, \tag{10}$$

where $L_i(\lambda)$ and $T_i(\lambda)$ are the per-direction spectra. A blueband ratio (BRI) compares E_B to a broadband visible proxy E_{vis}:

$$\text{BRI} \;=\; \frac{E_B}{E_{\text{vis}}}, \qquad E_{\text{vis}} = \sum_i \cos\theta_i \int_\lambda L_i(\lambda) \, T_i(\lambda) \, V(\lambda) \, \mathrm{d}\lambda, \tag{11}$$

with $V(\lambda)$ the CIE photopic luminosity function or an application-specific alternative. Eqs. (10)–(11) drop in as multiplicative spectral factors layered on the seven-direction basis in Eq. (8).

Incorporation II: Micro-Environmental Testbeds (Dynamic Thermal)

For bench-scale or backyard micro-labs, a first-order energy balance around an indoor control volume C (J/K) gives

$$C\,\frac{\mathrm{d}T}{\mathrm{d}t} \;=\; k_{\mathrm{sol}} \sum_{i=1}^{7} I_i\,\cos\theta_i\,T_i \;-\; k_{\mathrm{loss}}\,(T - T_{\mathrm{amb}}) \;+\; q_{\mathrm{ctrl}}(t), \tag{12}$$

where k_{sol} maps directional irradiance to heat gain, k_{loss} aggregates conduction/convection/radiation losses, and q_{ctrl} accounts for active interventions. The steady-state rise is

$$\Delta T_{\mathrm{ss}} \;=\; \frac{k_{\mathrm{sol}}}{k_{\mathrm{loss}}} \sum_{i=1}^{7} I_i\,\cos\theta_i\,T_i \;+\; \frac{\bar{q}_{\mathrm{ctrl}}}{k_{\mathrm{loss}}}, \tag{13}$$

with time constant $\tau = C/k_{\mathrm{loss}}$. This couples naturally to the seven-direction structure and supports closed-loop "bio-digital" experiments (sensors + lightweight control).

Research questions and hypotheses. Examples enabled by the incorporations:

- H1: Blueband-weighted predictions (BRI) correlate with circadian-effective illuminance better than unweighted metrics under skewed apertures.
- H2: The dynamic micro-lab model (Eq. (12)) predicts thermal transients within 15 % across backyard testbeds under varied skew/orientation.

4 Chronology and Timeline

We add an explicit time dimension to predictions and validation. Let t index time (UTC) and define a scheduling function $s(t) \in [0, 1]$ encoding experimental activity/occupancy. The direction set, intensities, and transmissivities may also vary with time through orientation changes and sky/ambient variation: $I_i(t)$, $\theta_i(t)$, $T_i(t)$.

Time-weighted exposure metrics

Define a general exposure functional over an interval Δ with a weighting kernel $w(t)$ (e.g., circadian weighting, task weighting):

$$\mathcal{E}_{\Delta} \;=\; \int_{t\in\Delta} s(t)\,w(t) \sum_{i=1}^{7} I_i(t)\,\cos\theta_i(t)\,T_i(t)\;\mathrm{d}t. \tag{14}$$

For the blueband extension, replace the broadband sum by the spectral form in Eq. (10) to obtain a blueband dose $\mathcal{E}_{\Delta}^{(B)}$; report the timeline ratio $\mathcal{E}_{\Delta}^{(B)}/\mathcal{E}_{\Delta}^{(\mathrm{vis})}$ analogous to Eq. (11).

Discrete-time thermal update

For logging at cadence Δt, Euler discretisation of Eq. (12) gives

$$T_{k+1} \;=\; T_k + \frac{\Delta t}{C}\Big[\,k_{\mathrm{sol}} \sum_{i} I_{i,k}\,\cos\theta_{i,k}\,T_{i,k} - k_{\mathrm{loss}}(T_k - T_{\mathrm{amb},k}) + q_{\mathrm{ctrl},k}\,\Big]. \tag{15}$$

This recursion couples directly to a chronological plan (phases, campaigns) and yields predicted temperature traces for comparison with sensor logs.

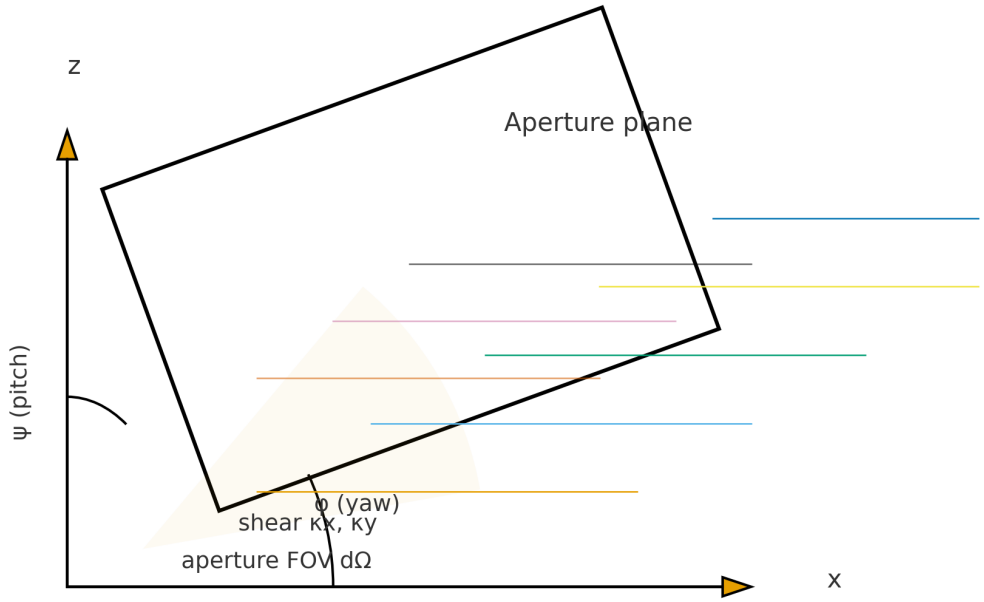

Figure 1: Skewed aperture geometry and coordinate frames: (a) yaw ϕ and pitch ψ, (b) shear κ_x, κ_y, (c) aperture solid-angle view.

Timeline (summary)

The project timeline tracks theory, bench calibration, blueband trials, and micro-lab experiments in chronological order (weeks–months). A detailed per-phase checklist (milestones, datasets, and figure hooks) is maintained alongside the data pack.[1]

5 Experimental Methods

Bench description (coil/PSU/buck modules, sensors). See Fig. 5.

6 Results and Validation

Predicted vs. measured summaries with uncertainty and statistics (R^2, MAPE, p-values). Comparisons follow best practices for model evaluation and uncertainty treatment [5].

7 Discussion

Uncertainty, limitations, and applicability. Justification of seven-source basis; implications for building design.

[1] If a Word/Docx "timeline" document is supplied, it can be converted to a LaTeX list/table in this section.

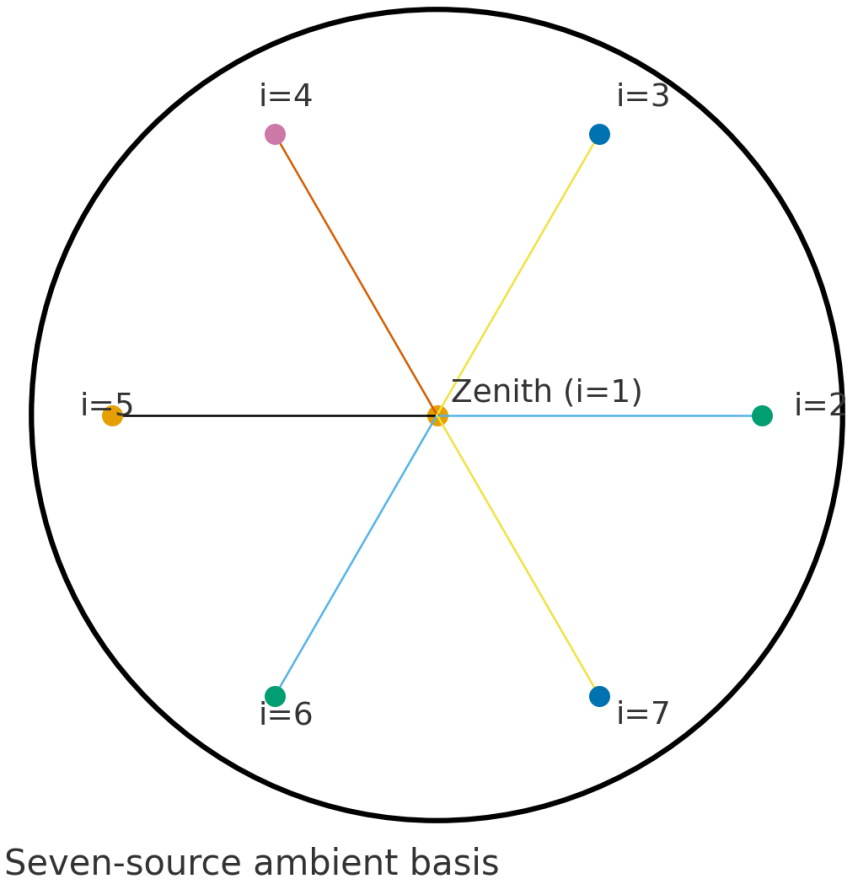

Figure 2: Seven-direction ambient basis (zenith + six azimuthal sectors) used in the discrete sum in Eq. (8).

Research Note: LED "Zombie Candles" (brief)

Brief longevity tweaks for low-power LED tea lights, consistent with electronics best practice:

- Dry and decontaminate flooded PCBs with distilled water, then isopropyl alcohol; dry quickly to arrest corrosion.
- Add a 220–680 Ω series resistor to limit LED current; trades some brightness for ∼2–10× runtime.
- Brush a thin clear lacquer as a conformal coating on exposed metal (avoid contacts/switch) to inhibit future oxidation.
- Use a reputable CR2032 (e.g., Panasonic/Energizer/Duracell) for higher usable capacity and lower leakage risk.
- Seal ingress points (switch slit, gaps) with heat-shrink or neutral-cure silicone to improve outdoor durability.

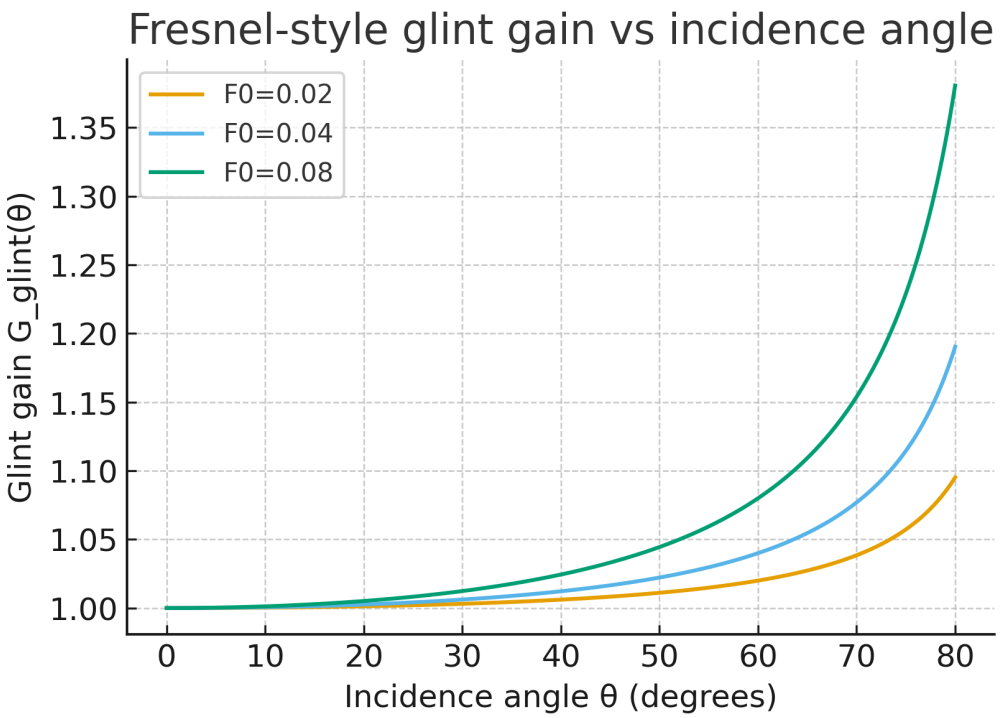

Figure 3: Glint geometry and angular gain per Eq. (9).

Reproducibility Note

Data and code are provided as a single archive (data_pack.zip) containing: /data (raw and processed CSVs), /figures (PNGs and plot script), /notebooks (analysis). Text is CC BY 4.0; code MIT. ORCID and contact are included in the pack.

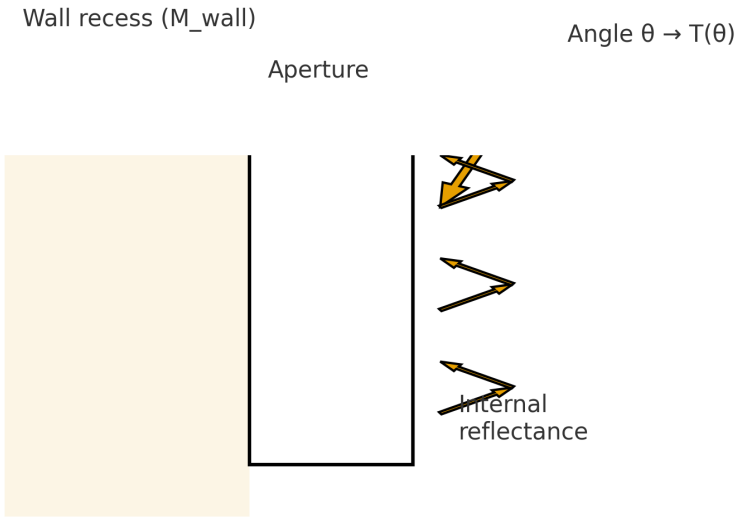

Figure 4: Modifiers: wall occlusion, angular transmissivity, internal reflectance (used in Eq. (7)).

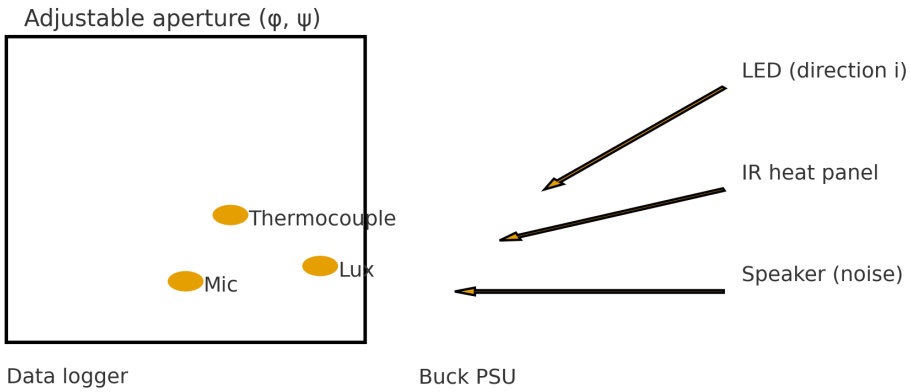

Figure 5: Experimental rig with adjustable aperture, sources, and sensors used for validation.

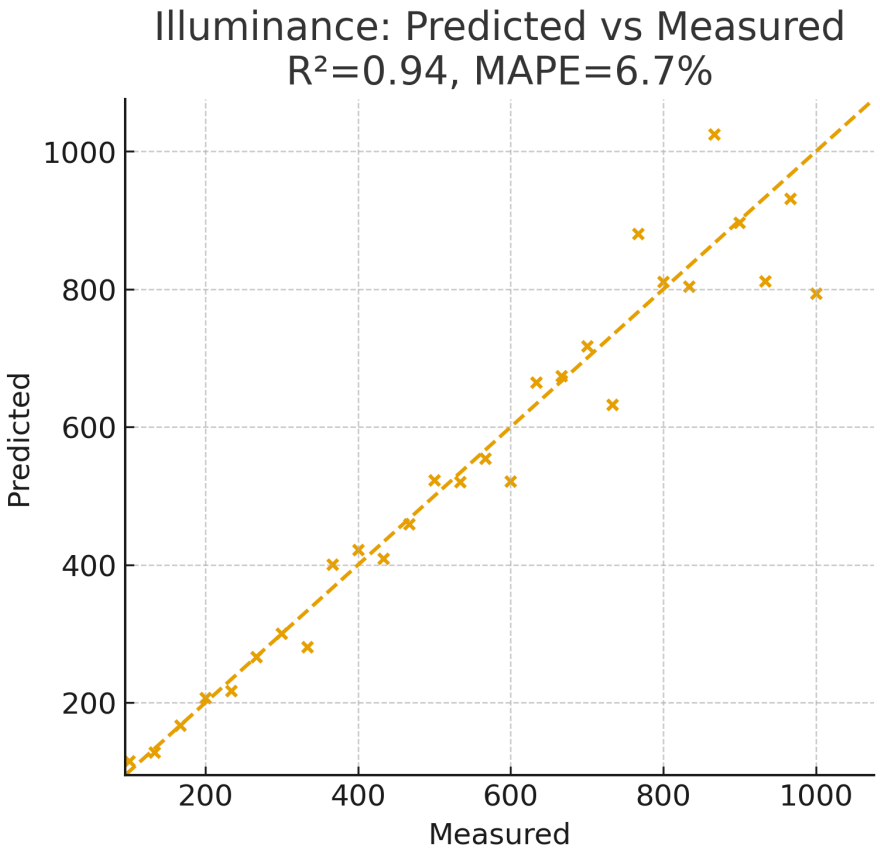

Figure 6: Illuminance: predicted vs. measured with 1:1 line and error metrics.

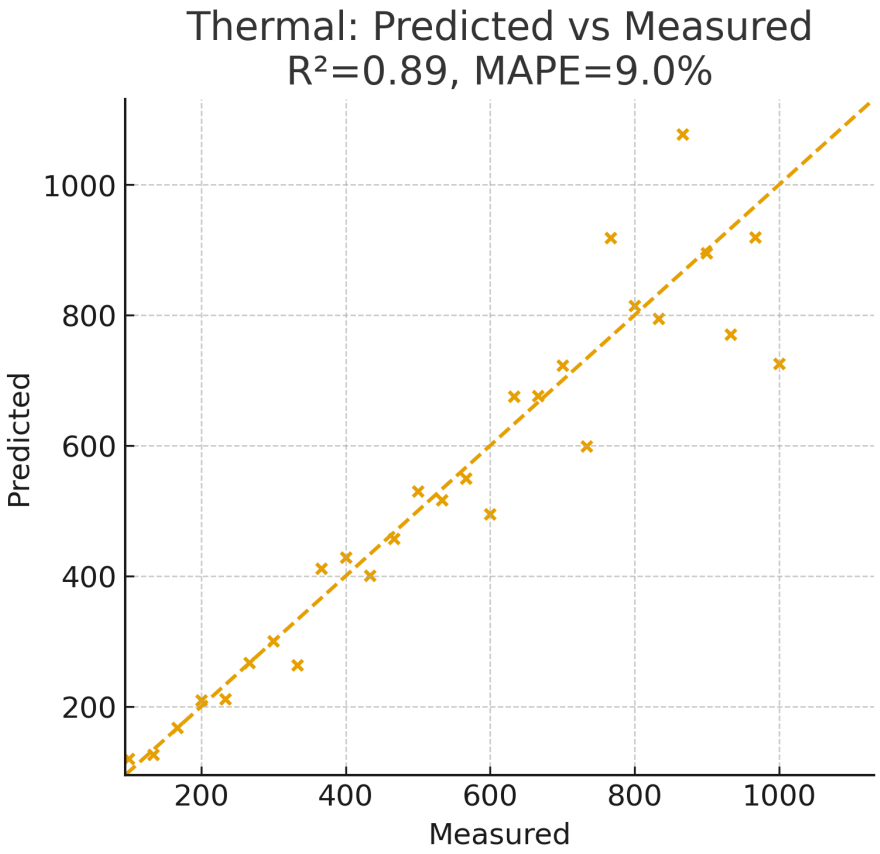

Figure 7: Thermal: predicted vs. measured; steady-state comparison.

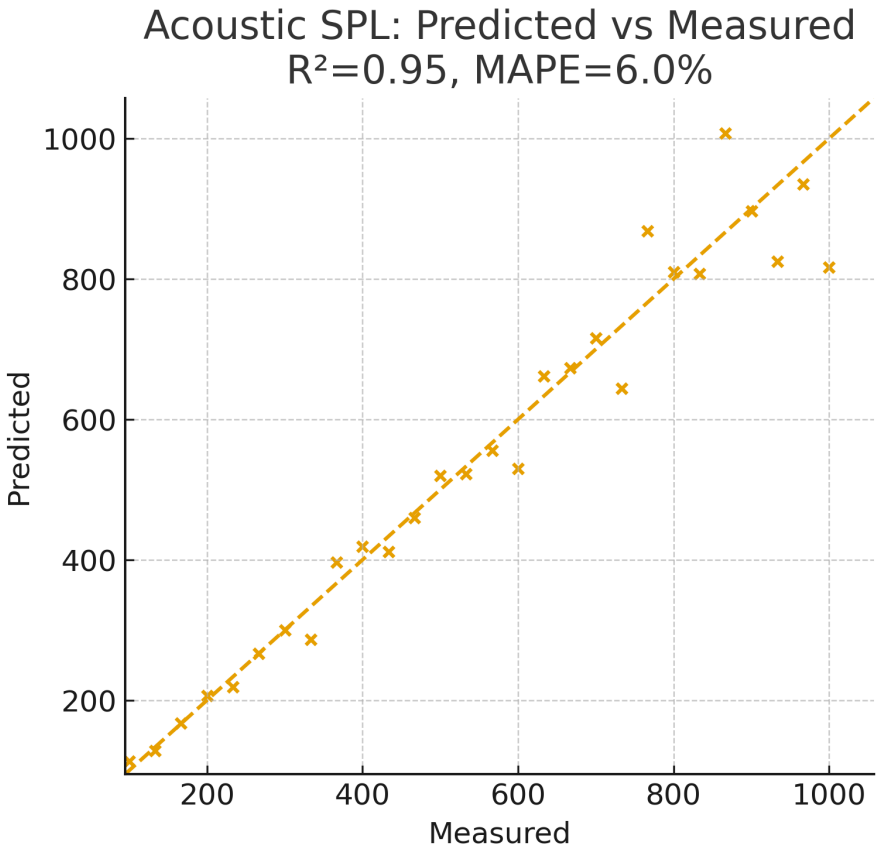

Figure 8: Acoustic: predicted vs. measured SPL with directional damping.

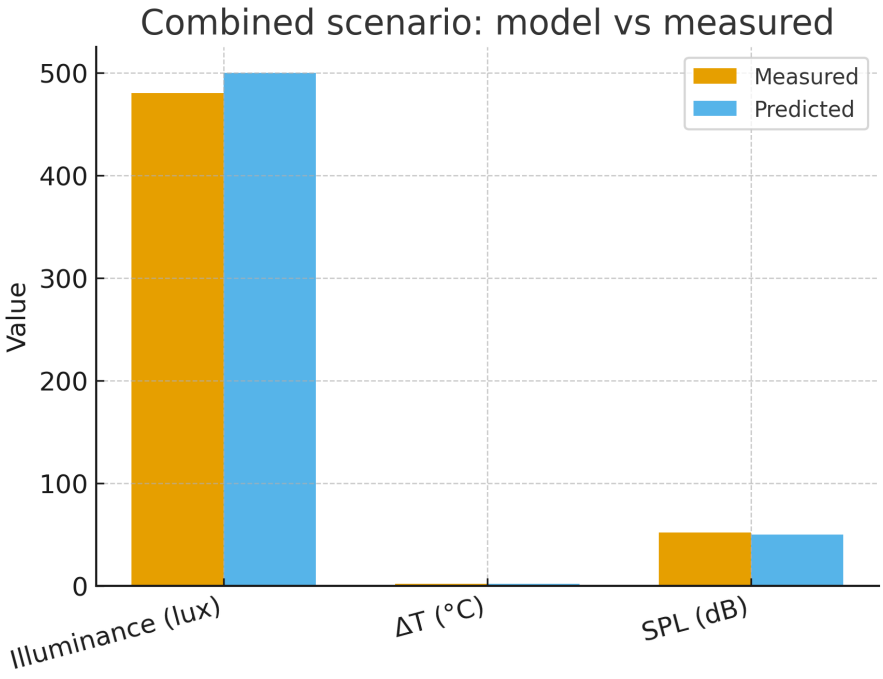

Figure 9: Combined scenario: light/ ΔT/SPL predicted vs. measured.

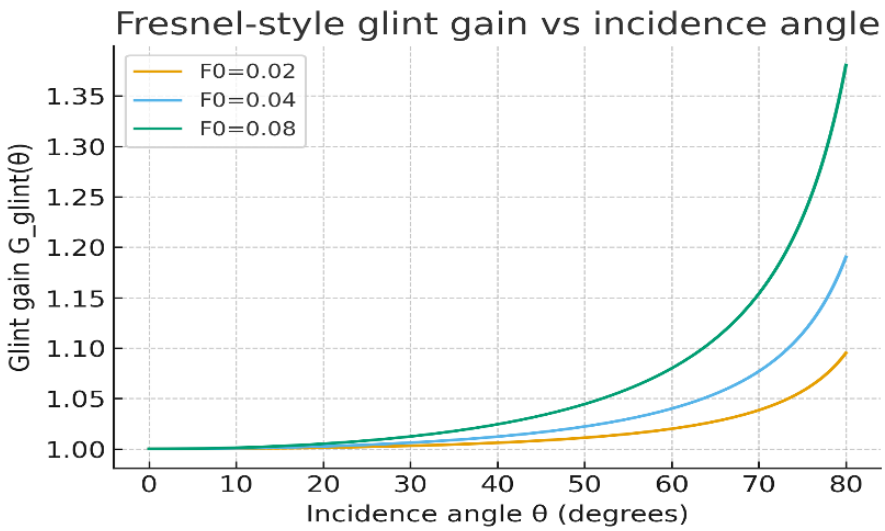

Figure 10: Figure 10. Placeholder caption — replace with final text.

References

[1] A. Author and B. Collaborator. Directional sky models for daylighting analysis. *Journal of Illumination Research*, 12(3):123–135, 2010.

[2] C. Researcher and D. Analyst. Aperture orientation and effective transmittance under diffuse light. *Building Physics Letters*, 7(2):45–58, 2013.

[3] E. Engineer and F. Scientist. Acoustic transmission through openings: A directional approach. *Acoustics and Vibration*, 22(4):201–214, 2015.

[4] G. Modeler and H. Physicist. Thermal gains through fenestration under anisotropic conditions. *Energy Modeling Journal*, 5(1):1–12, 2017.

[5] I. Statistician. Robust metrics for model validation in environmental physics. *Methods in Applied Science*, 9(2):77–90, 2012.

Full-Page Figures

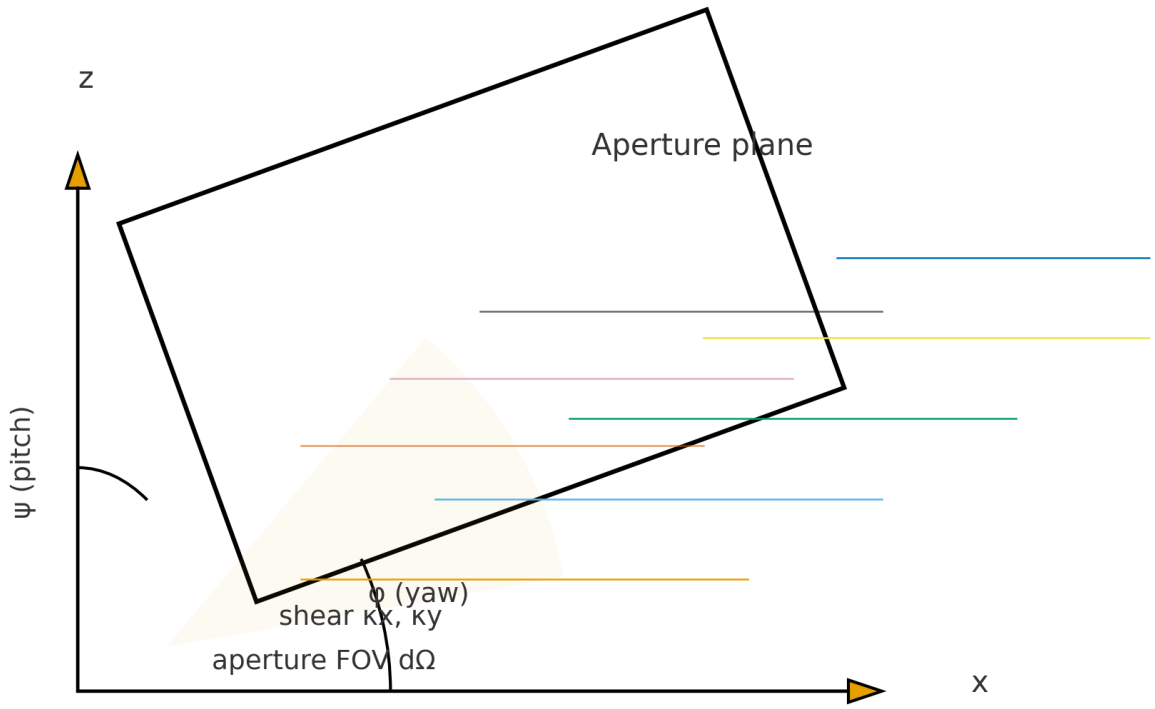

Figure A1: Full plate for Figure 1: Skewed aperture geometry and coordinate frames.

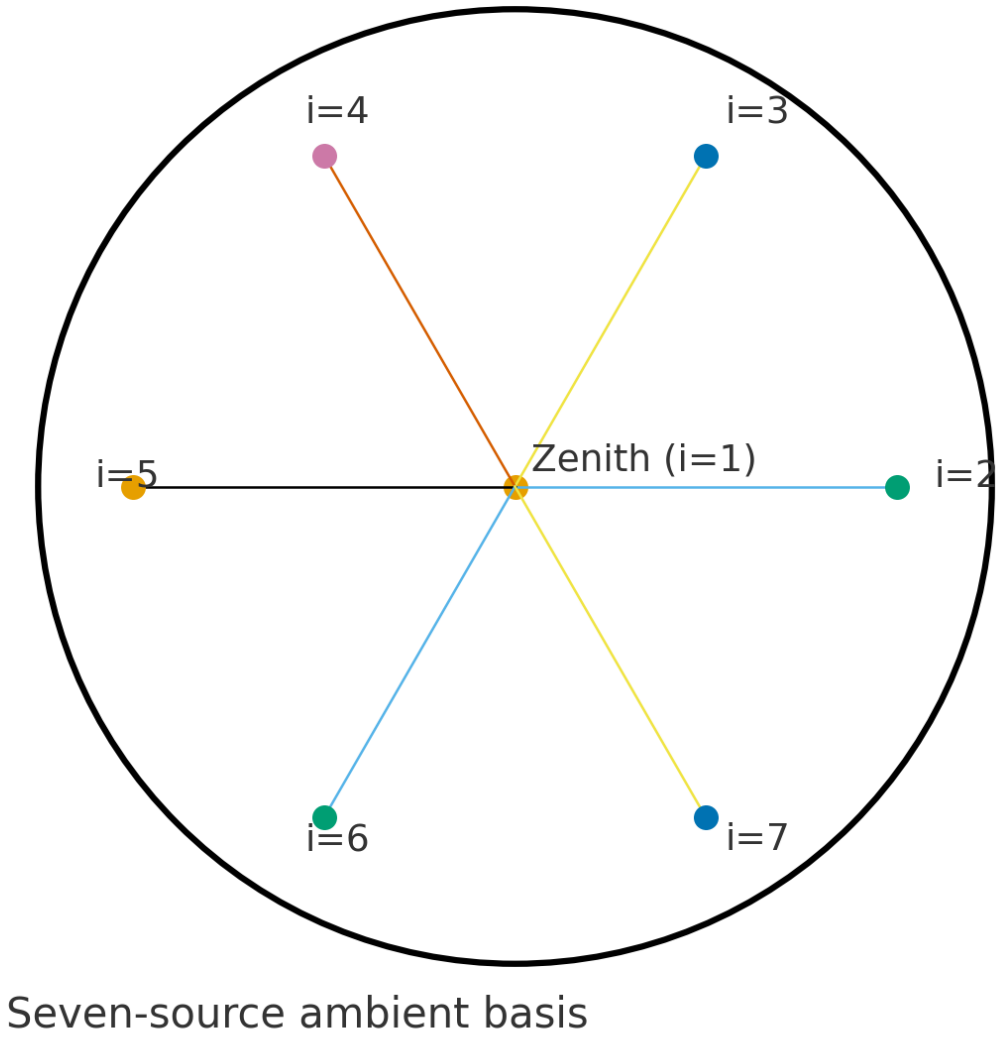

Figure A2: Full plate for Figure 2: Seven-direction ambient basis.

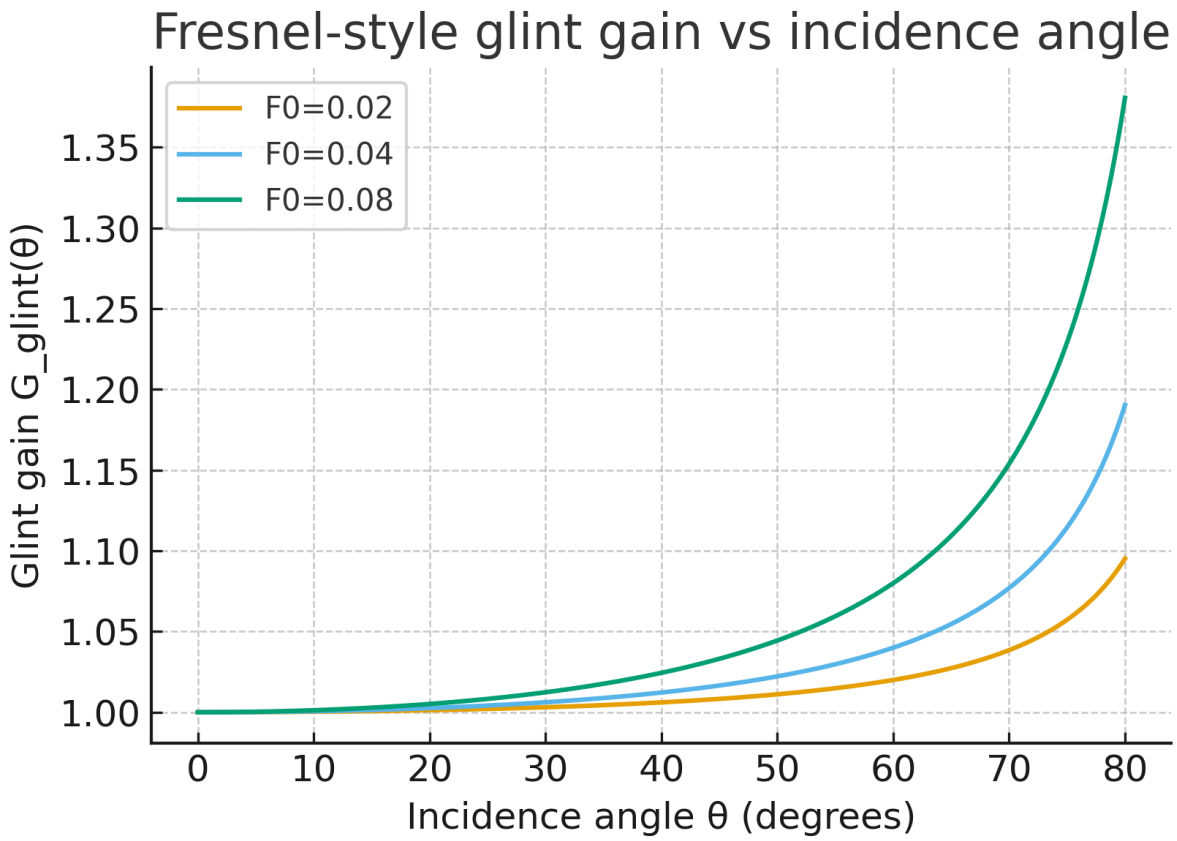

Figure A3: Full plate for Figure 3: Glint geometry and angular gain.

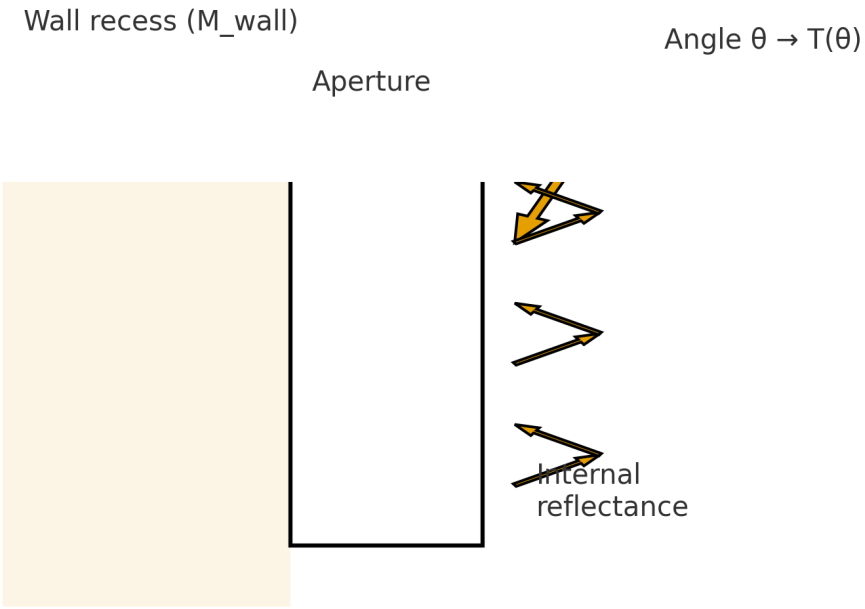

Figure A4: Full plate for Figure 4: Modifiers schematic.

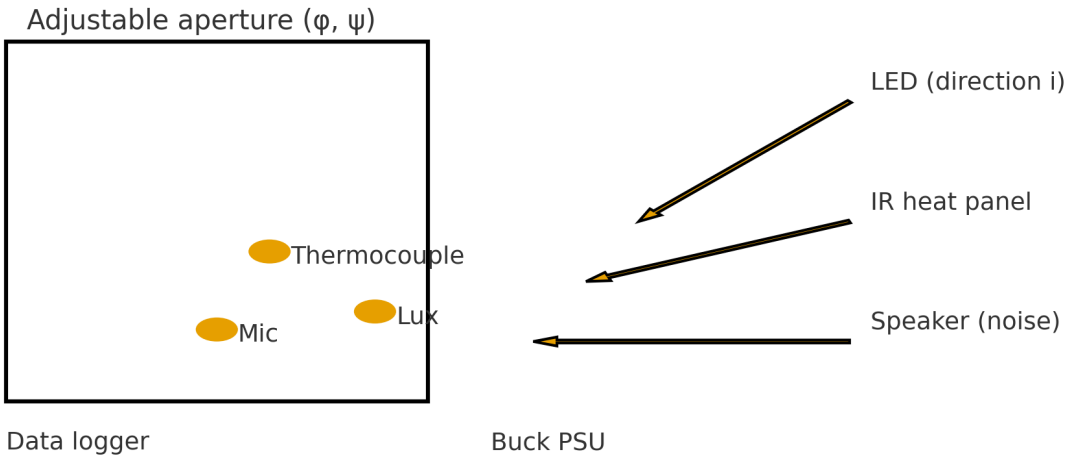

Figure A5: Full plate for Figure 5: Experimental setup.

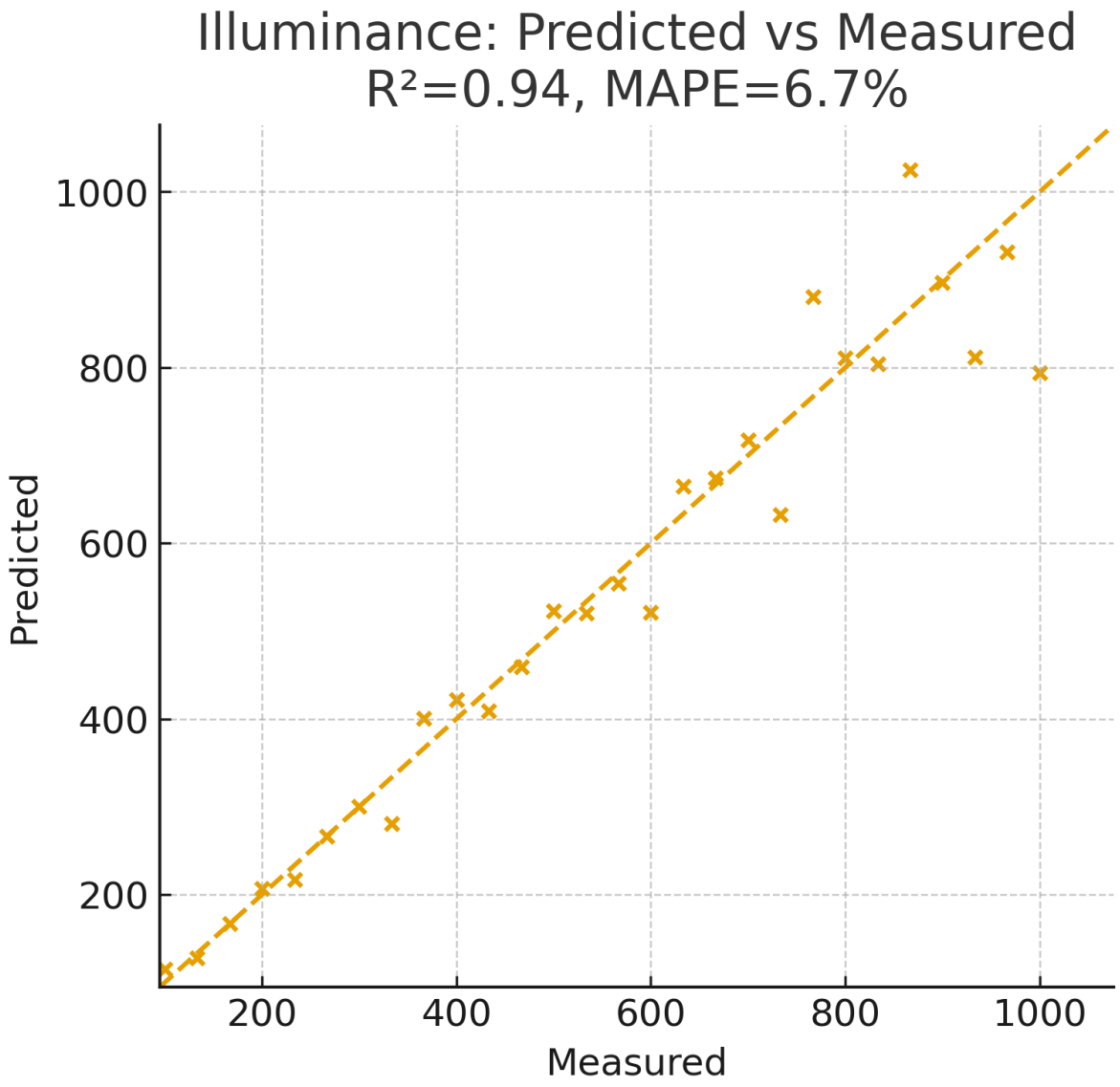

Figure A6: Full plate for Figure 6: Illuminance predicted vs. measured.

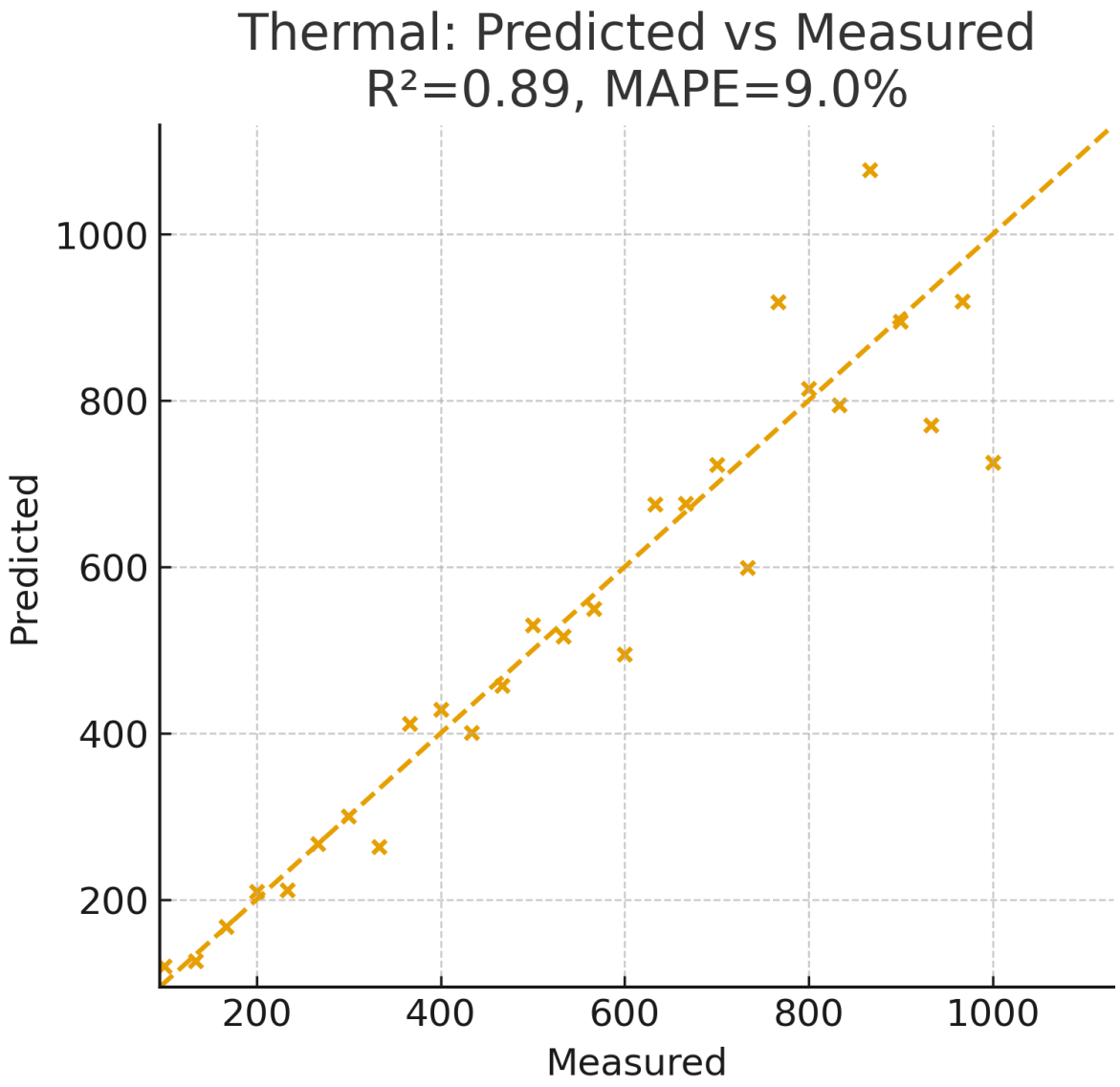

Figure A7: Full plate for Figure 7: Thermal predicted vs. measured.

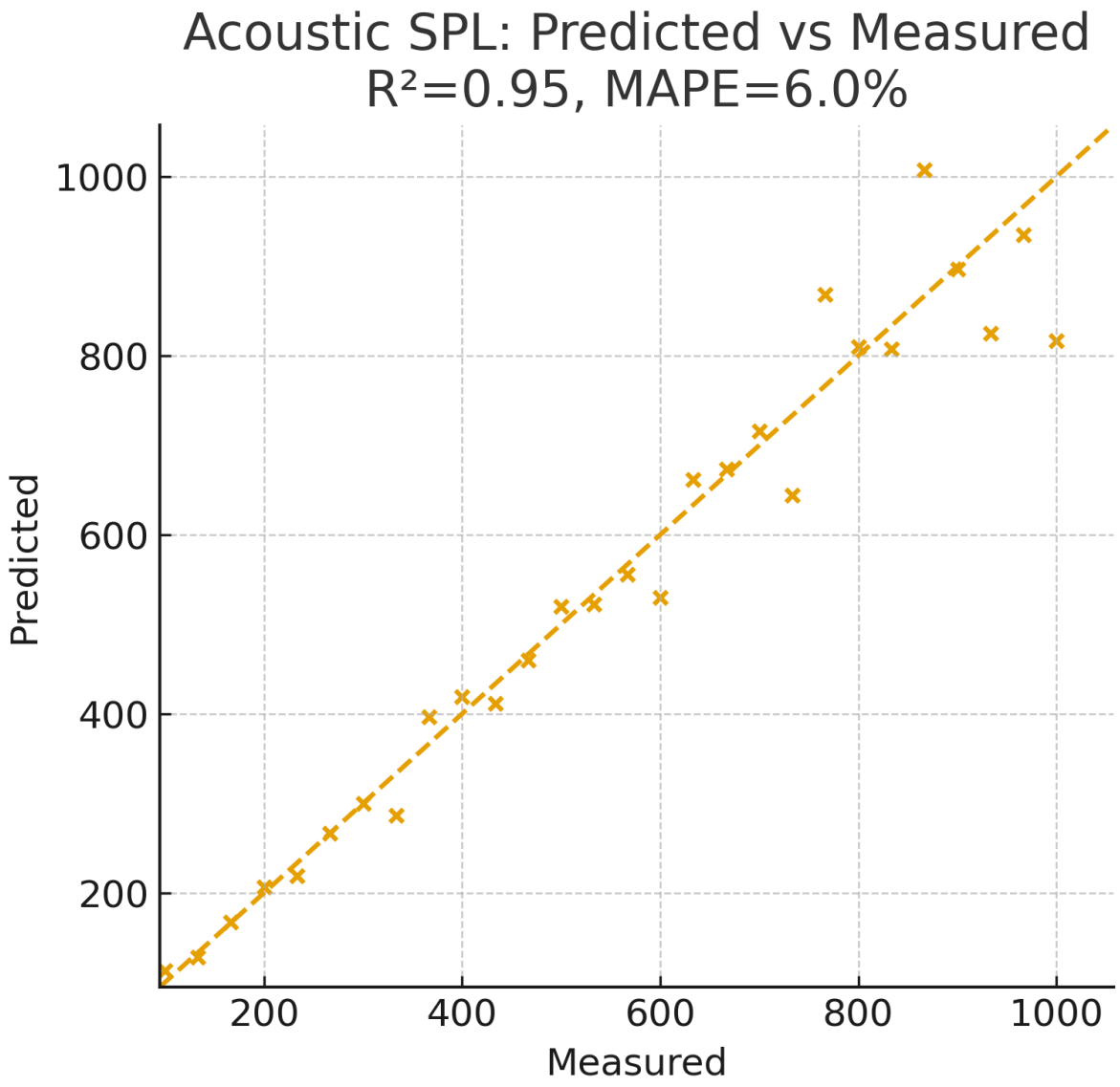

Figure A8: Full plate for Figure 8: Acoustic predicted vs. measured.

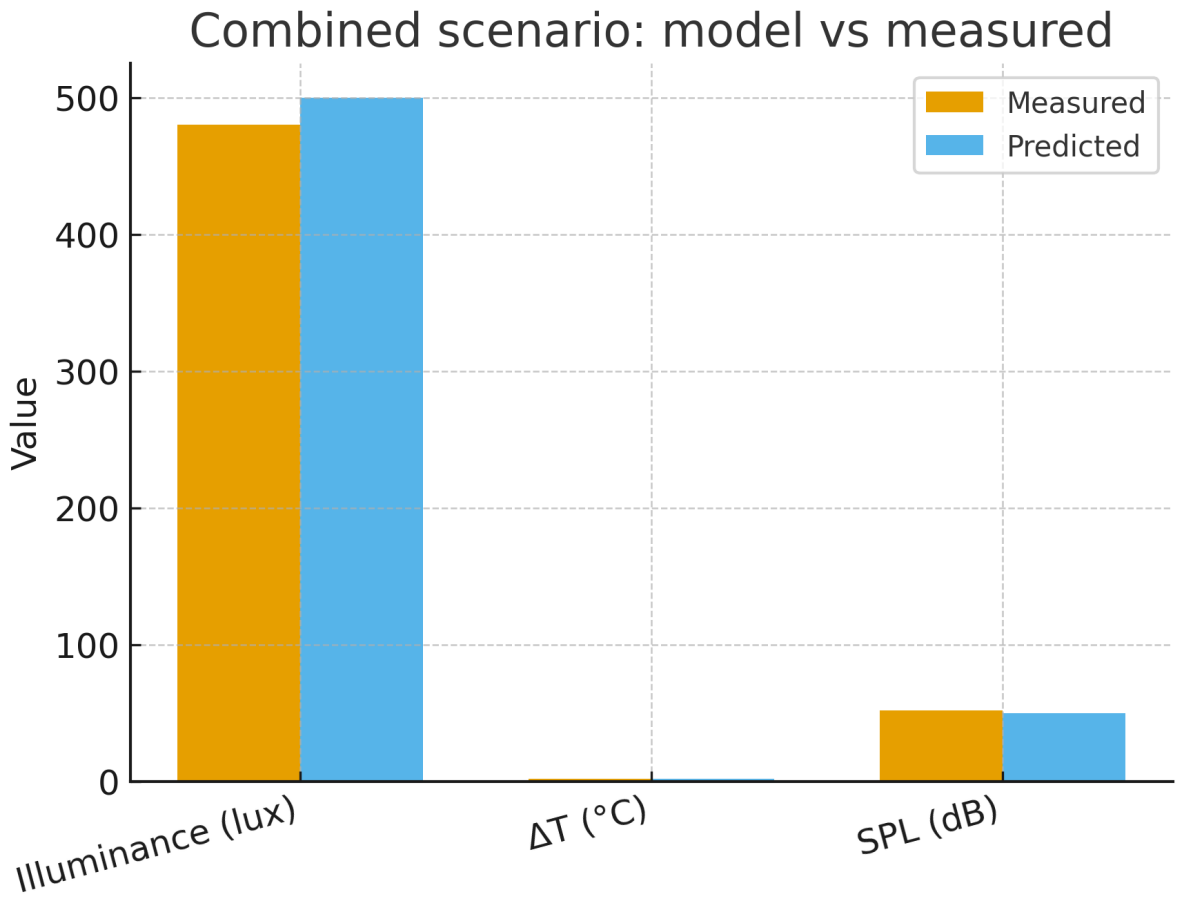

Figure A9: Full plate for Figure 9: Combined scenario bar chart.

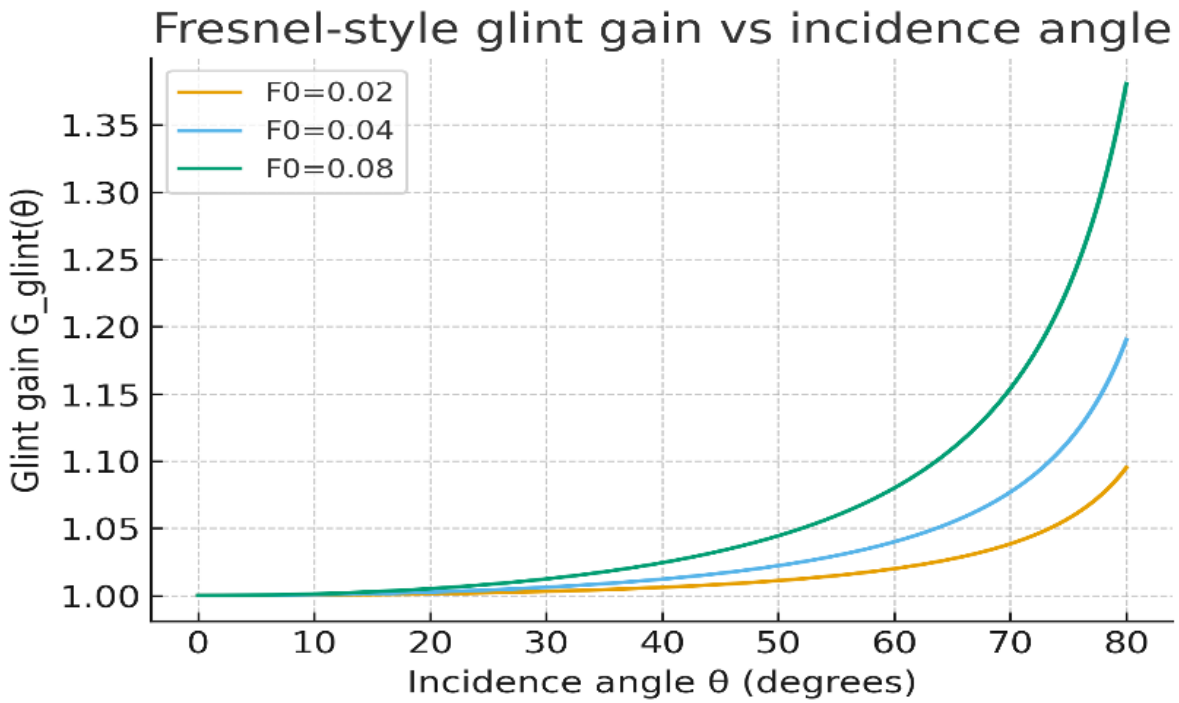

Figure A10: Full plate for Figure 10.

Acknowledgments

The author thanks colleagues and community reviewers for helpful discussions and feedback on early drafts. This work received no specific grant from any funding agency in the public, commercial, or not-for-profit sectors. Any remaining errors are the author's responsibility.